



TITLE:

Using multiple sensors to detect uncut crop edges for autonomous guidance systems of head-feeding combine harvesters

AUTHOR(S):

Cho, Wonjae; Iida, Michihisa; Suguri, Masahiko; Masuda, Ryohei; Kurita, Hiroki

CITATION:

Cho, Wonjae ...[et al]. Using multiple sensors to detect uncut crop edges for autonomous guidance systems of head-feeding combine harvesters. Engineering in Agriculture, Environment and Food 2014, 7(3): 115-121

ISSUE DATE:

2014-07

URL:

<http://hdl.handle.net/2433/189413>

RIGHT:

© 2014 Asian Agricultural and Biological Engineering Association. Published by Elsevier B.V.; This is not the published version. Please cite only the published version.; この論文は出版社版ではありません。引用の際には出版社版をご確認ご利用ください。

Using Multiple Sensors to Detect Uncut Crop Edges for Autonomous Guidance Systems of Head-Feeding Combine Harvesters

Wonjae CHO^{*1}, Michihisa IIDA^{*2}, Masahiko SUGURI^{*3},
Ryohei MASUDA^{*3}, Hiroki KURITA^{*3}

Abstract

This study proposes a method for detection of uncut crop edges using multiple sensors to provide accurate data for the autonomous guidance systems of head-feeding combine harvesters widely used in the paddy fields of Japan for harvesting rice. The proposed method utilizes navigation sensors, such as a real-time kinematic global positioning system (RTK-GPS), GPS compass, and laser range finder (LRF), to generate a three-dimensional map of the terrain to be harvested at a processing speed of 35 ms and obtain the crop height. Furthermore, it can simultaneously detect the uncut crop edges by RANdom SAmple Consensus (RANSAC). The average of the lateral offset value and crop height of the uncut crop edge detected by the proposed method were 0.154 m and 0.537 m, respectively.

[Keywords] Head-feeding combine harvester, Uncut crop edge detection, RTK-GPS, GPS compass, Laser range finder

I Introduction

Crop harvesting in a field environment requires a high level of concentration because the operator has to simultaneously control the travel speed and direction of the harvesting machine while adjusting the height of the header after considering numerous parameters including crop height, biomass density, and other terrain conditions. However, it is challenging for the operator to maintain his or her health and physical condition because of the long hours operating the harvester under unfavorable environmental conditions such as the dust particles suspended in midair and noise and vibrations generated from the machine while harvesting. To overcome this challenge, autonomous guidance systems that perform the required tasks without human control are being developed to automatically steer the unmanned harvesters along the edges of uncut crops.

In contrast to a system that helps the operator control the harvesting during operation by guiding the harvesting machine along the prearranged target path, the autonomous guidance system performs unmanned harvesting and can be used to replace all field operations performed by the operator (Kise *et al.*, 2005). The autonomous guidance system does not rely on the experience and proficiency of the operator and is able to

enhance work stability and productivity because the system allows the harvesting machine to automatically travel fast and accurately along the target path while harvesting as it detects the surrounding environment. The autonomous guidance system utilizes the following functions for unmanned travel and harvesting. First, by using the navigation sensors mounted on the harvesting machine, the current position of the harvester is estimated in real-time and uncut crop edges are detected by sensing the surrounding environment. Next the target path is determined together with the travel direction and speed of the harvesting machine, which allows the harvesting machine to travel and perform tasks without damaging the crops. Finally, the harvest machine is automatically steered, precisely running on the planned target path. To fulfill these functions, the autonomous guidance system requires on-board navigation sensors and methodologies satisfying the sensor characteristics to provide guidance information that can be used for path planning and accurate steering.

In recent years, numerous sensor methodologies that utilize various navigation sensors have been proposed and developed for an autonomous guidance system of harvesting machines, for example, global positioning systems (GPSs), machine vision, laser range finders

^{*1} JSAM Student Member, Graduate School of Agriculture, Kyoto University, Kitashirakawa Oiwake-cho, Sakyo-ku, Kyoto, 606-8502, Japan; cho@elam.kais.kyoto-u.ac.jp

^{*2} JSAM Member, Corresponding author, Graduate School of Agriculture, Kyoto University, Kitashirakawa Oiwake-cho, Sakyo-ku, Kyoto, 606-8502, Japan; iida@elam.kais.kyoto-u.ac.jp

^{*3} JSAM Member, Graduate School of Agriculture, Kyoto University, Kitashirakawa Oiwake-cho, Sakyo-ku, Kyoto, 606-8502, Japan

(LRFs), contact, and azimuth. The researchers at the National Agricultural Research Center (Japan) and Mitsubishi Farm Machinery Co., Ltd., developed an automatic traveling control system that can follow crop rows and turn at the end of rows by detecting the uncut crops with a contact sensor and gyroscope mounted on head-feeding combine harvesters (Sato *et al.*, 1996). A team of researchers from the Carnegie-Mellon University and National Aeronautic and Space Administration (NASA) used a color camera mounted on a hay windrower to develop an automated guidance system that can travel and perform harvesting tasks along the uncut crop edges detected in real-time, which was successfully tested for harvesting in a field of alfalfa (Ollis and Stentz, 1997). Scientists at Cemagref (France) proposed an automatic guidance method that used laser sensors mounted on both windrow and combine harvesters (Chateau *et al.*, 2000). Benson *et al.* (2003) used a monochrome camera mounted on a head directly above the uncut crop edge to develop and demonstrate a machine-vision-based guidance system for small-grain harvesters that can automatically steer by detecting uncut crop edges. Rovira-Más *et al.* (2007) proposed a method for detecting uncut crop edges that used stereoscopic vision for an autonomous guidance system for corn harvesters. The researchers at Kyoto University developed an autonomous guidance system that plans the target path and automatically steers using a real-time kinematic global positioning system (RTK-GPS) and GPS compass mounted on a head-feeding combine harvester along with the field information obtained prior to the harvest (Iida *et al.*, 2012). The harvesting performance of the system was successfully tested in a paddy field.

These earlier researchers proposed sensor methodologies that can successfully detect uncut crop edges from the sensory data by using the inherent characteristics of sensors and applying them to the autonomous guidance systems. However, the sensor methodologies proposed by these researchers have limitations, depending on sensor characteristics. In the studies that utilized machine vision and LRFs mounted on harvesters for the detection of uncut crop edges (Ollis and Stentz, 1997; Chateau *et al.*, 2000; Benson *et al.*, 2003; Rovira-Más *et al.*, 2007), the positions of the detected uncut crop edges were identified in relation to the mounted sensors. However, because the absolute position of the harvester could not be obtained from the mounted sensors, the locations of the detected uncut crop edges in the field were not identifiable. On the contrary,

in a study that configured the autonomous guidance system by mounting on the harvester RTK-GPS detectors that could acquire absolute positions (Iida *et al.*, 2012), the location of the harvester could be identified in the field. However, because information about the upcoming harvesting environment could not be acquired, the actual harvesting was only limited to following pre-specified paths.

To overcome the above constraints, this paper proposes a method that uses multiple sensors to detect uncut crop edges to provide data for autonomous guidance systems of head-feeding combine harvesters that are widely used in Japan for the harvesting of rice and wheat crops. At a rapid processing speed of 35 ms, the proposed method uses navigation sensors, such as an RTK-GPS, a GPS compass, and an LRF, mounted on a head-feeding combine harvester to provide the current position of the machinery and a three-dimensional (3D) map of the terrain to be harvested, which are needed for planning of the target path. Moreover, the uncut crop areas can be separated from the ground areas, and the edge and height of the uncut crops can be determined from the generated 3D map data.

II Materials and Methods

1. Experimental setup

(1) Navigation sensors

The navigation sensors used for this study were an RTK-GPS (Topcon Co., Ltd., Legacy-E+), a GPS compass (Hemisphere Co., Ltd., V110), an LRF (SICK AG, LMS111) and machine vision (Sensor Technology Co., Ltd., STC-TC33USB). As shown in Fig. 1, the navigation sensors (an RTK-GPS antenna and GPS compass) were mounted on the roof, the LRF was mounted on the upper front, and machine vision was installed in the ceiling inside the operation room of the head-feeding combine harvester (Mitsubishi Agricultural Machinery Co., Ltd., VY50CLAM). The sensors serve the following functions.



CHO, IIDA, SUGURI, MASUDA, KURITA :

Using Multiple Sensors to Detect Uncut Crop Edges for Autonomous Guidance Systems of Head-Feeding Combine Harvesters³

Fig. 1 Navigation sensors mounted on the head-feeding combine harvester (modified from Iida *et al.*, 2012).

An RTK-GPS was used to obtain the absolute and accurate position of the head-feeding combine harvester. To compensate for the signal errors generated by the sensors, a virtual reference station (VRS) system was used. A personal digital assistance device (HewlettPackard Co., Ltd., iPAQ hx2190b) and mobile phone (Docomo Co., Ltd., FOMA P2403), both installed with global navigation satellite system software, were used as reference stations. Using the VRS RTK method, a positioning accuracy of up to $\pm 3\text{cm}$ was achieved.

A GPS compass was used to obtain the heading information of the head-feeding combine harvester and consisted of various components, such as dual GPS antennas, a differential GPS beacon module, a single-axis gyro, and a tilt sensor. Although the GPS heading information was typically used as a primary information source, backup heading information obtained from the gyro and tilt sensors could also be used in instances where the main source could not be accessed because of signal blockings. The heading information accuracy of the GPS compass was within 0.50° RMS.

An LRF was used to obtain the profile information of the terrain to be harvested by the head-feeding combine harvester. The LRF performed two-dimensional (2D) scanning and its technical specifications are shown in Table 1. For this experiment, the field of view (90°), angular resolution (0.25°), and rotation frequency (25 Hz) were set as intrinsic parameters of the LRF.

Table 1 Technical specification of the LRF.

Model	LMS111
Maximum field of view ($^\circ$)	270
Angular resolution ($^\circ$)	0.25, 0.50
Maximum scanning range (m)	20
Rotation frequency (Hz)	25, 50
Data interface type	Ethernet, RS-232, CAN

Although machine vision was not used for the detection of uncut crop edges, it was used for visual recording and storing of the traveling and harvesting tasks of the head-feeding combine harvester. The machine vision used in this study used CCD image sensors and supports a USB 2.0 interface. The sensor also acquired color images with a 640 pixels (horizontal) by 480 pixels (vertical) resolution, at a speed of 10 FPS. The lens (Pentax Ricoh Imaging Co., Ltd., FL-CC815B-VG) installed on the machine vision system

had a field of view of 56.5° . For this study, the acquired color images were saved in the audio video interactive format.

(2) Control system

Two electronic control units (ECU), named ECU-KU1 and ECU-KU2, were developed to integrate the control of the components of the head-feeding combine harvester and the navigation sensors mounted on the harvester, and the pre-existing control system for the head-feeding combine harvester was remodeled (Iida *et al.*, 2012). As shown in Fig. 2, ECU-KU1 communicates with the components of the head-feeding combine harvester, and ECU-KU2 with the navigation sensors (RTK-GPS and GPS compass). ECU-KU1 and ECU-KU2 communicate with one another via the control area network bus. The personal computer (PC) used for integrated system control communicates with ECU-KU1 via the RS-232C ports, while the LRF communicates with the PC via Ethernet, and the machine vision via USB port.

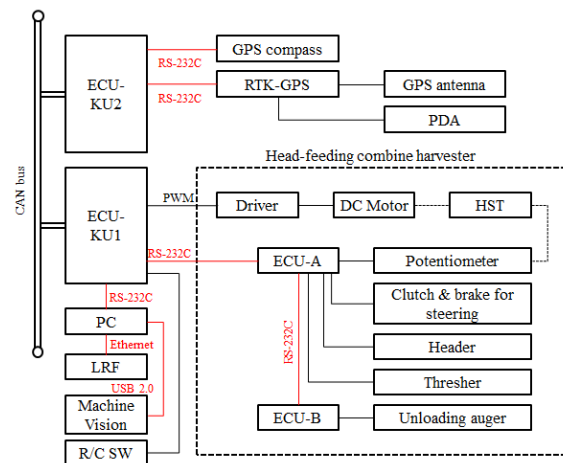


Fig. 2 Control system architecture of head-feeding combine harvester.

(3) Integrated sensor control platform

The study implemented a guidance method using multiple sensors by introducing the integrated sensor control platform (ISCP), currently developed by our project team for head-feeding combine harvesters. ISCP supports various navigation sensors, such as machine vision, LRFs, and GPSs that are mainly used for the autonomous guidance systems of head-feeding combine harvesters, and they can also display real-time sensor data with a graphical user interface. In addition, the open-source platform can be freely modified and re-distributed without license restrictions (<https://github.com/FiroKyoto/IntegratedSensorControlPlatform.git>).

In this study, ISCP was used to obtain data about the components and navigation sensors of the head-feeding combine harvester from ECU-KU1, ECU-KU2, the machine vision, and LRF at a frequency of 10 Hz.

2. 3D terrain mapping

Because rice is planted evenly in 0.3 m inter-row (d_r) and 0.2 m intra-row (d_c) intervals in the paddy fields of Japan, as shown in Fig. 3, each row is parallel to its neighbors. Because the head-feeding combine harvester performs its harvesting task while traveling along the uncut crop edge, the precise detection of the crop edge is pivotal to the performance enhancement of the autonomous guidance system. The 2D profile data from the LRF, the heading angle data from the GPS compass, and the absolute position data from the RTK-GPS, all obtained from the sensors mounted on the head-feeding combine harvester, were used to generate a 3D map of the to be harvested terrain and to obtain location of the uncut crop edge and crop height.

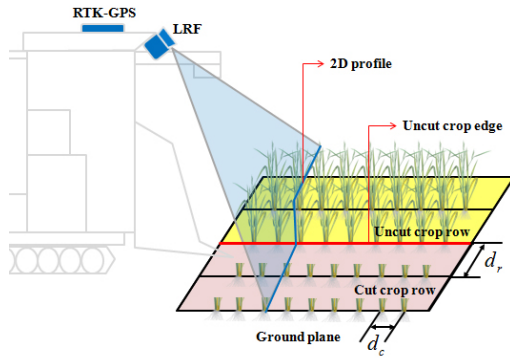
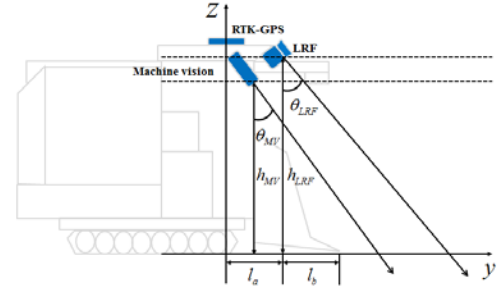


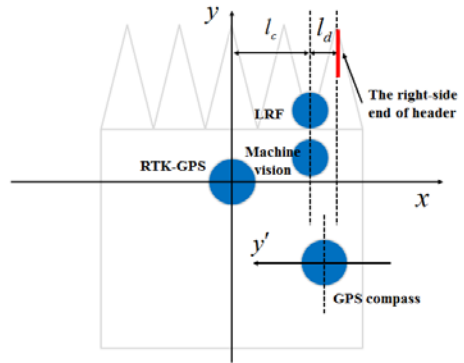
Fig. 3 Rows of rice plants in a paddy field.

Fig. 4 depicts the extrinsic parameters of the navigation sensors mounted on the head-feeding combine harvester. Parameters θ_{LRF} and h_{LRF} are defined as the tilt angle and height of the installed LRF from the ground, which are 50.5° and 2.5 m, respectively. The longitudinal distance (l_a) and transverse distance (l_c) of the LRF from the origin of the xy plane of the 3D Euclidean space ($W = \{(x, y, z)\} \in E^3$), configured with the center of the RTK-GPS as the base point, are 0.45 m and 0.59 m, respectively. Moreover, the longitudinal distance (l_b) and transverse distance (l_d) of the divider of the right-side end of the header from the center of the LRF are 0.6 m and 0.07 m, respectively. The GPS compass is installed in parallel to the xy plane of W space and calculates the angle between the GPS compass in the clockwise direction, which is aligned to the magnetic north direction of the

Earth, and the y' axis. Therefore, the heading angle (φ) of the head-feeding combine harvester can be obtained by adding $+90^\circ$ to the angle obtained above. The center of the lens installed as part of the machine vision is located 2.3 m perpendicular to the ground surface (h_{MV}) at a tilt angle (θ_{MV}) of 38.5° . Moreover, because the machine vision is positioned on the yz plane, together with the LRF, both centers of the machine vision lens and LRF are positioned on the yz plane.



(a) yz plane.



(b) xy plane.

Fig. 4 Extrinsic parameters of the navigation sensors.

During the process of transformation and integration, a 3D terrain map is generated from the data acquired by the navigation sensors mounted on the head-feeding combine harvester, and it has the mathematical relationship, as shown in Fig. 5.

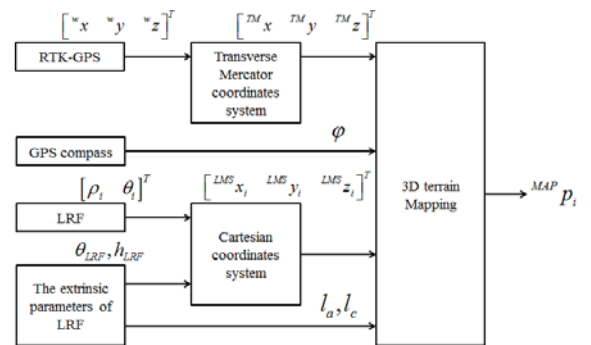


Fig. 5 Mathematical relationship between sensors.

CHO, IIDA, SUGURI, MASUDA, KURITA :

Using Multiple Sensors to Detect Uncut Crop Edges for Autonomous Guidance Systems of Head-Feeding Combine Harvesters⁵

1 First, the data in the polar coordinates system acquired
2 from the LRF and extrinsic parameters (θ_{LRF}, h_{LRF}) of
3 the LRF are substituted in Eq. (1), and then converted
4 into data in the Cartesian coordinates system, which can
5 be expressed in W space. Next, the absolute position
6 data acquired from the RTK-GPS is converted to data in
7 the transverse mercator coordinates system, which
8 assumes the absolute position of the RTK-GPS mounted
9 on the harvester at the beginning of the harvesting task as
10 the center of origin. Lastly, the sensory data converted by
11 the above process, heading angle (φ) of the harvester,
12 and extrinsic parameters (l_a, l_c) of the LRF are
13 substituted in Eq. (2) and then converted into data in the
14 Cartesian coordinates system, which can be expressed in
15 W space. The converted data is consecutively saved in a
16 dynamic array until the head-feeding combine harvester
17 reaches the end of the row.

$${}^{LMS}p_i = \begin{bmatrix} {}^{LMS}x_i \\ {}^{LMS}y_i \\ {}^{LMS}z_i \end{bmatrix} = \begin{bmatrix} \rho_i \cos \theta_i \\ \rho_i \sin \theta_i \sin \theta_{LRF} \\ h_{LRF} - \rho_i \sin \theta_i \cos \theta_{LRF} \end{bmatrix} \quad (1)$$

where

θ_i is the measurement angle acquired from the LRF,
 ρ_i is the reflection distance acquired from the LRF,
and θ_{LRF} and h_{LRF} are the tilt angle and the height
of the LRF from the ground, respectively.

$${}^{MAP}p_i = \begin{bmatrix} {}^{MAP}x_i \\ {}^{MAP}y_i \\ {}^{MAP}z_i \end{bmatrix} = \begin{bmatrix} {}^{TM}x \\ {}^{TM}y \\ {}^{TM}z \end{bmatrix} + \begin{bmatrix} \cos \varphi & \sin \varphi & 0 \\ -\sin \varphi & \cos \varphi & 0 \\ 0 & 0 & 1 \end{bmatrix} \begin{bmatrix} l_c + {}^{LMS}x_i \\ l_a + {}^{LMS}y_i \\ {}^{LMS}z_i \end{bmatrix} \quad (2)$$

where

${}^{TM}x, {}^{TM}y, {}^{TM}z$ are values acquired from the
RTK-GPS converted into values in the transverse
mercator coordinates system, φ is the heading angle
of the head-feeding combine harvester, and l_a and
 l_c are the longitudinal and transverse distances from
the RTK-GPS to the LRF.

18 The LRF data transformed into Cartesian coordinate
19 system data was used for the discrimination of the 3D
20 points generated into the uncut crop and ground areas.
21 Because the head-feeding combine harvester performed
22 harvesting while traveling counter clockwise in this
23 study, the uncut crop area was located on the left side
24 and the ground area on the right side of the border points
25 obtained from the LRF data. Fig. 6 explains the
26 distribution of the LRF data expressed on the xz plane
27 of space W . Leveraging such characteristics, segment
28 l_{hn} connects at point p_h where z of the LRF dataset
29 (${}^{LMS}p_i$) becomes maximum, with the end points (p_n)
30 calculated, as well as point (p_k), where the length (d_k) of

31 the perpendicular to the data set and the segment
32 becomes maximum, by using Eq. (3) (Kimberling, 1998).
33 Because the resulting p_k denotes the outermost
34 boundary point of the uncut crop area, as shown in Fig. 6,
35 the uncut crop area and ground area can be discriminated
36 based on p_k .

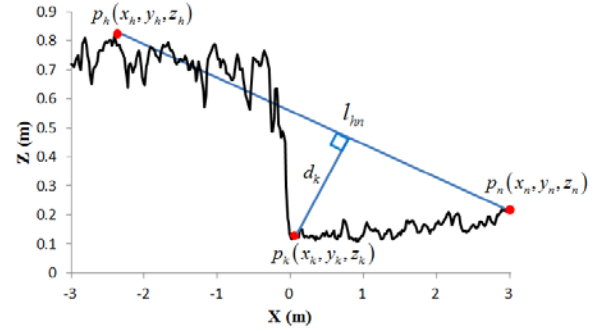


Fig. 6 LRF data distribution expressed on xz plane.

$$d_k = \frac{|(x_n - x_h)(z_h - z_k) - (x_h - x_k)(z_n - z_h)|}{\sqrt{(x_n - x_h)^2 + (z_n - z_h)^2}} \quad (3)$$

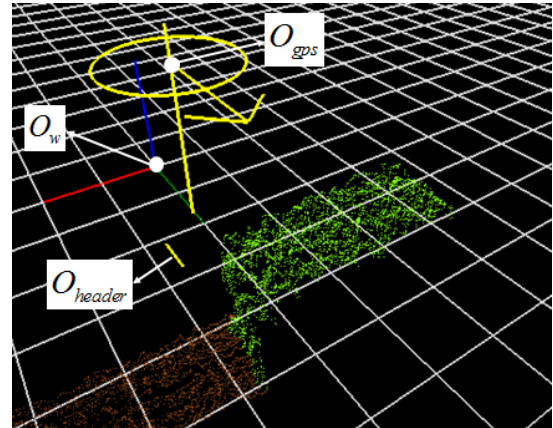


Fig. 7 3D terrain map using OpenGL.

41 Fig. 7 shows the 3D terrain map obtained when
42 applying the proposed method. The 3D terrain map is
43 expressed by using Open Graphics Library (OpenGL)
44 application programming interface (API). OpenGL is an
45 API that performs the rendering of 3D objects, such as
46 lines, rectangles, and other primitive graphic elements,
47 and projects the results onto a 2D screen (Shreiner, 2009).
48 Every time ${}^{MAP}p_i$ data is added onto the dynamic array,
49 which is used for storing ${}^{MAP}p_i$, the glVertex3f function,
50 which is provided for the conversion of the data into 3D
51 point expression in OpenGL, is used to express in
52 real-time the data value of ${}^{MAP}p_i$ in the 3D point format
53 in space W of OpenGL. O_w signifies the coordinate
54 system of space W , which is configured using the

1 absolute position obtained from the RTK-GPS at the start
2 of harvesting as the origin. O_{gps} and O_{header} refer to
3 the center of the RTK-GPS and right-side end of the
4 header, respectively. Additionally, the 3D points of the
5 uncut crops and ground are expressed in green and
6 brown, respectively.

3. Uncut crop edge detection

9 For the detection of the uncut crop edge from the 3D
10 terrain map generated in real-time, the study utilized
11 RANdom SAMple Consensus (RANSAC). The
12 RANSAC algorithm predicts the model parameters from
13 the original data that has severe measurement noise
14 (Fischler and Bolles, 1981). RANSAC randomly
15 performs samplings of the minimum data required for
16 determining the model parameters from the total original
17 data and calculates the values repeatedly to find the
18 optimal values.

19 The original data applied to the RANSAC algorithm is
20 the previously calculated set of the outermost boundary
21 points (p_k) of the uncut crop area, configured in a
22 dynamic array. The dynamic array is initialized at the
23 start of harvest and consecutively adds p_k until the
24 head-feeding harvester reaches the end of the row. In this
25 case, z values from p_k are not used because the uncut
26 crop edge exists on the xy plane of space W .
27 Furthermore, p_k is determined as an inlier where the
28 perpendicular distance value of p_k to the direct line of
29 the model is smaller than the threshold value and an
30 outlier if bigger. In this study, the threshold value was set
31 as 0.1. The number of repeats (\bar{N}) of the RANSAC
32 algorithm can be calculated from Eq. (4). In this study,
33 \bar{N} was determined by setting the number of sample data
34 (\bar{m}) as 5, the probability (\bar{p}), where at least one sample
35 set included valid data, such as 0.99, and the probability
36 ($\bar{\mu}$) of the data validity as 0.5. The RANSAC algorithm is
37 then given as follows:

RANSAC algorithm

```
1 Initial: A set of  $N$  points in dynamic array
2 repeat
3   Choose a sample of  $m$  points uniformly at random
4   Fit a straight line model through the  $m$  points
5   Compute the perpendicular distance of other points
   to the straight line model
6   Construct the inlier set
7   If there are enough inliers, re-compute the straight
   line model parameters, store the straight line, and
   remove the inliers from the set
```

```
8 until Maximum  $\bar{N}$  iterations reached
9 return Best-fit straight line model
```

$$\bar{N} = \frac{\log(1 - \bar{p})}{\log(1 - \bar{\mu}^{\bar{m}})} \quad (4)$$

40
41 Fig. 8 shows the results of determining the uncut crop
42 edge from the 3D terrain map by using the RANSAC
43 algorithm. The uncut crop edge was determined and
44 updated by the RANSAC algorithm every time
45 additional data was received from the navigation sensors
46 until the head-feeding combine harvester reached the end
47 of the row. As can be observed in Fig. 8, the uncut crop
48 edge is expressed as a red line on the 3D terrain map,
49 which can be accurately determined by RANSAC.

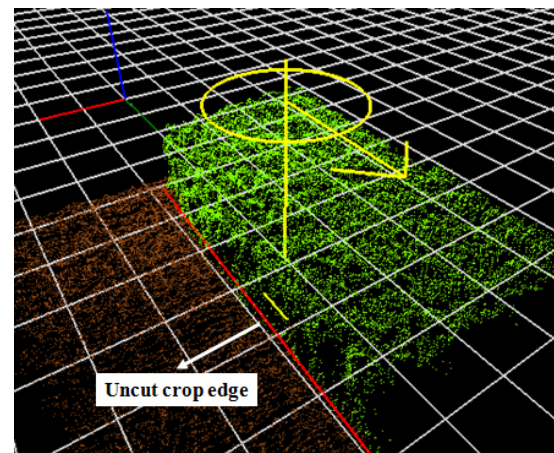


Fig. 8 Uncut crop edge detection by RANSAC.

4. Experimental method

54 To evaluate the performance of the proposed method,
55 data from the navigation sensors were obtained during
56 the harvest operations of a head-feeding combine
57 harvester controlled by an operator in a rice paddy field
58 in Nantan City, Kyoto Prefecture, Japan. The
59 head-feeding combine harvester harvested rice along
60 target paths at an average travel speed of 0.6 m/s.
61 Because the head-feeding combine harvester performed
62 its operations while traveling counter clockwise, as
63 shown in Fig. 9, the sensor data obtained were
64 categorized into four datasets according to the movement
65 directions.

66 In this study, the proposed method was used to
67 evaluate the performance of the determination of the
68 uncut crop edge from each section. First, target paths that
69 functioned as the baseline for each determination zone
70 were set. Then, the lateral offset was calculated between
71 the determined uncut crop edges and baseline target
72 paths. As shown in Fig. 9, the target path for each zone is

CHO, IIDA, SUGURI, MASUDA, KURITA :

Using Multiple Sensors to Detect Uncut Crop Edges for Autonomous Guidance Systems of Head-Feeding Combine Harvesters⁷

1 a single straight line, which is derived by connecting the
2 3D points on the right-side end of the headers expressed
3 on the 3D terrain map at the beginning and end-of-row
4 time points of the harvesting task. Because the straight
5 line is expressed on the xy plane, z values are not used
6 from the 3D points obtained above. To derive the target
7 path from each harvest zone, an experienced operator
8 accurately operated the combine in a paddy field filled
9 with rice plants planted at regular intervals. The combine
10 traveled at a speed of 0.6 m/s, lower than the normal
11 harvest travel speed of 1.0 m/s, and followed the uncut
12 crop row to perform the harvesting task.

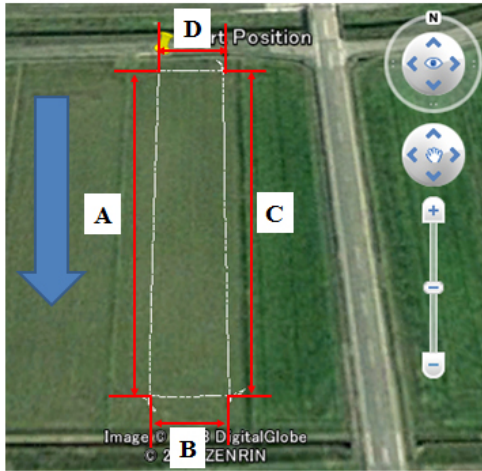


Fig. 9 Traveling path of the head-feeding combine harvester (image from Google Maps).

III Results and Discussion

18 Fig. 10 shows the result of a 3D terrain map generated
19 with the navigation sensor data obtained using the
20 proposed method. The movie clip of the results can be
21 accessed via the following address (<http://youtu.be/juy-YuOfvgkk>). The proposed method, at an average
22 processing speed of 35 ms, acquires data from the
23 mounted sensors, generates a 3D terrain map by using
24 the sensory data, and simultaneously determines the
25 uncut crop edge and average crop height from the 3D
26 terrain map.

28 The average crop height obtained for each harvest
29 section under the proposed method and lateral offset
30 values of the target path to the determined uncut crop
31 edge are summarized in Table 2. Fig. 11 shows the target
32 paths set for each section as well as the result of the
33 uncut crop edge determined by RANSAC. The target
34 path and the uncut crop edge are expressed as blue and
35 red lines, respectively, while the set of boundary points
36 applied by RANSAC are shown in gray. In Fig. 11, the
37 x -axis refers to the distance traveled by the head-feeding

38 combine harvester while performing the harvesting task,
39 starting from the absolute position acquired from the
40 RTK-GPS mounted on the head-feeding combine
41 harvester at the start of the harvest as the center of origin.
42 The y -axis signifies the perpendicular distance from the
43 determined values (the set of boundary points and uncut
44 crop edge) to the assumed target path, obtained by using
45 the proposed method. Regarding the signs of y -axis
46 values, they will be negative ($-$) when the determined
47 values are located on the left side of the target path in the
48 traveling direction of the head-feeding combine harvester
49 on the 3D terrain map, and positive ($+$) when located on
50 the right side of the target path. The lateral offset for
51 each zone, shown in Table 2, indicates the average of
52 y -axis values of the uncut crop edge, as shown in Fig. 11.
53 Moreover, the “average crop height” for each zone refers
54 to the average of the z values of the 3D points
55 (expressed in green in Fig. 10) that are distinguished as
56 uncut crop area of the generated 3D terrain map.

57 Table 3 shows the average perpendicular distances of
58 the determined uncut crop edge from the set of boundary
59 points used for RANSAC and the inlier ratio of the set of
60 boundary points for each harvest section. The inlier ratio,
61 shown in Table 3, refers to the ratio of the number of
62 elements out of the set of boundary points stored in the
63 dynamic array that have perpendicular distances to the
64 uncut crop edges within the inlier range. When the
65 perpendicular distance is smaller than the threshold value,
66 the boundary point is regarded as an inlier, and regarded
67 as an outlier if bigger. In this study, the threshold value
68 is set at 0.1 for the proposed uncut crop edge detection
69 method. As the value for the inlier ratio increase, the
70 number of elements out of the set of boundary points,
71 determined by RANSAC with the uncut crop edge as the
72 basis, is dispersed in high densities. As shown in Fig. 11,
73 the uncut crop edge determined for each section is
74 located on the right side of the target path, as viewed
75 from the perspective of the traveling direction of the
76 head-feeding combine harvester, and the average lateral
77 offset to the target path is 0.154 m.

Table 2 Results using the proposed method.

Dataset	Movement Direction	Average Crop Height [m]	Lateral Offset [m]
A	South	0.514	0.294
B	East	0.503	0.139
C	North	0.549	0.067
D	West	0.580	0.119
Average		0.537	0.154

Table 3 Average perpendicular distance and inlier ratio of the set of boundary points.

Dataset	Average Perpendicular Distance [m]	Inlier Ratio [%]
A	0.070	74.4
B	0.052	90.2
C	0.072	78.2
D	0.059	83.6
Average	0.063	81.6

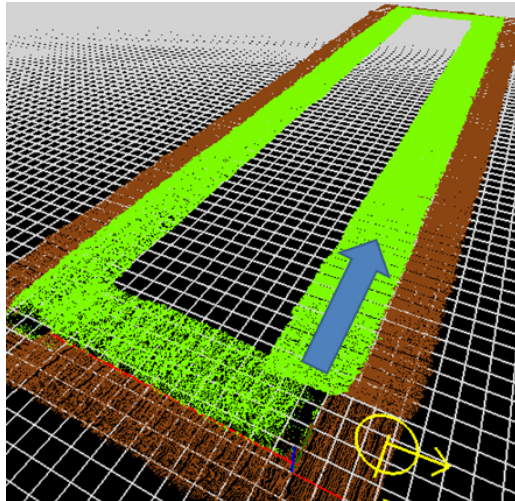
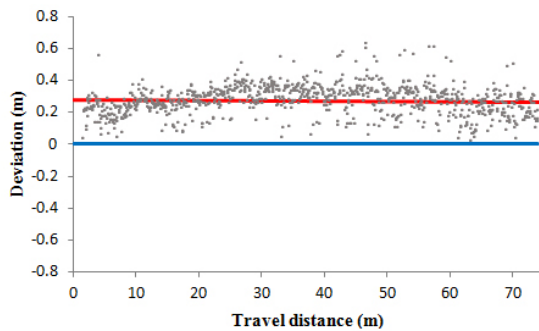
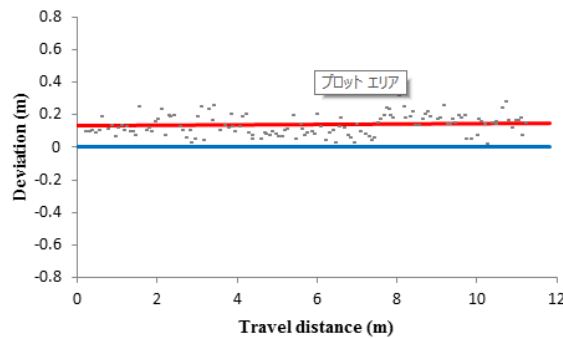


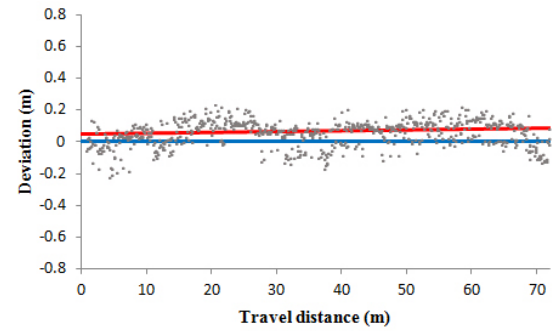
Fig. 10 3D terrain map of the experiment field.



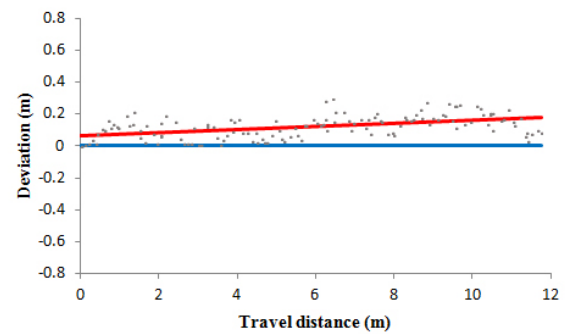
(a) Section A.



(b) Section B.



(c) Section C.



(d) Section D.

Fig. 11 Target path and the uncut crop edge determined by RANSAC.

The main reason for the lateral offset between the determined uncut crop edge and target path when applying the proposed method can be explained from Fig. 12. The paddy field image in Fig. 12 was acquired from the machine vision, which was mounted on the head-feeding combine harvester that was performing the harvest task in Section A. When performing the task in Section A, the harvester was operated accurately, following the target path (blue line), as perceived by an experienced operator. Therefore, the right-side end of the header can be considered to be located on the straight line of the target path, as shown in Fig. 12. Moreover, the red line shown in Fig. 12 signifies the row of crops already harvested that is located on the right-side of the target path. Because an inter-row interval of rice plants in a Japanese paddy field is 0.3 m, the lateral offset of the red line to the target path is 0.3 m. The lateral offset value between the determined uncut crop edge and target path in Section A is 0.294 m, which is almost identical to the lateral offset value (0.3 m) between the red line and the target path shown in Fig. 12. As described, the lateral offset is caused by the lodging of the uncut crops, which obscures the region between the target path and red line,

CHO, IIDA, SUGURI, MASUDA, KURITA :

Using Multiple Sensors to Detect Uncut Crop Edges for Autonomous Guidance Systems of Head-Feeding Combine Harvesters⁹

thereby making it difficult for the LRF to scan the region from the location where it is mounted (${}^{LRF}O_a$). To resolve the above issue, the mounting location of the LRF needs to be moved to the right-side (${}^{LRF}O_b$) on the right-side end of the header.

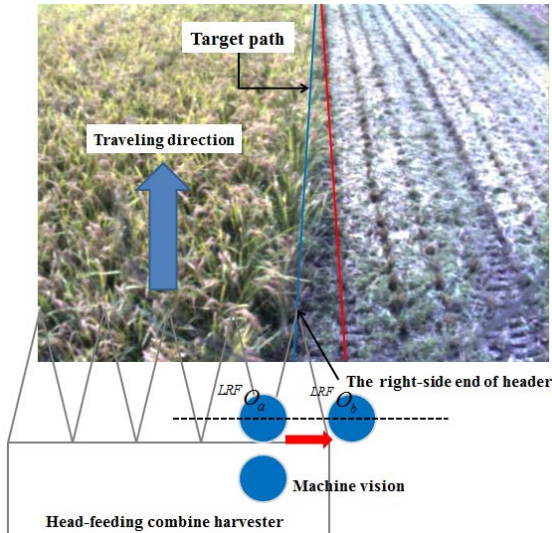


Fig. 12 Paddy field image acquired during harvesting task from Section A and relative position of the head-feeding combine harvester.

IV Summary and Conclusions

This study proposed a method to detect uncut crop edges using multiple sensors to provide accurate data for the autonomous guidance systems of head-feeding combine harvesters that are widely used in the paddy fields of Japan for harvesting rice. The proposed method was able to generate 3D maps of the terrain to be harvested at a processing speed of 35 ms by using navigation sensors, such as an RTK-GPS, a GPS compass, and an LRF. At the same time, the location of the uncut crop edge and crop height were obtained. The average of the lateral offset value and crop height of the uncut crop edge, determined by the proposed method, were 0.154 m and 0.537 m, respectively.

While the proposed method was robust in determining the uncut crop edge in general, its performance displayed a tendency to decline when the target path was obscured by the lodging of rice plants. Therefore, to enhance the performance of the proposed method, the mounting position of the LRF needs to be modified to allow for a more accurate scanning of the target path, together with the addition of an algorithm that can adjust for the error in results.

References

- Benson, E. R., J. F. Reid and Q. Zhang. 2003. Machine vision-based guidance system for agricultural grain harvesters using cut-edge detection. *Biosystems Engineering* 86(4): 389-398.
 - Chateau, T., C. Debain, F. Collange, L. Trassoudaine and J. Alizon. 2000. Automatic guidance of agricultural vehicles using a laser sensor. *Computers and Electronics in Agriculture* 28(3): 243-257.
 - Fischler, M. A. and R. C. Bolles. 1981. Random sample consensus: a paradigm for model fitting with applications to image analysis and automated cartography. *Communications of the ACM* 24(6): 381-395.
 - Iida, M., R. Uchida, H. Zhu, M. Suguri, H. Kurita and R. Masuda. 2012. Path-following control for a head-feeding combine robot. *Engineering in Agriculture, Environment and Food* 6(2): 61-67.
 - Kimberling, C. 1998. Triangle centers and central triangles: Utilitas Mathematica Publishing, Inc.
 - Kise, M., Q. Zhang and F. Rovira Más. 2005. A stereovision-based crop row detection method for tractor-automated guidance. *Biosystems Engineering* 90(4): 357-367.
 - Ollis, M. and A. Stentz. 1997. Vision-based perception for an automated harvester. In *Proc. IEEE/RSJ International Conference on Intelligent Robots and Systems*, 1838-1844. September.
 - Rovira-Más, F., S. Han, J. Wei and J. F. Reid. 2007. Autonomous guidance of a corn harvester using stereo vision. *Agricultural Engineering International: the CIGR Ejournal* 9.
 - Sato, J., K. Shigeta and Y. Nagasaka. 1996. Automatic operation of a combined harvester in a rice field. In *Proc. IEEE/SICE/RSJ International Conference on Multisensor Fusion and Integration for Intelligent Systems*, 86-92. Washington, DC, 8-11 December.
 - Shreiner, D. 2009. *OpenGL programming guide: The official guide to learning OpenGL, Versions 3.0 and 3.1*: Pearson Education.
- (Received : X. January. 20XX, Accepted : X. February. 20XX)